

Structure and magnetism of Fe mono- and multi-layer systems as seen by conversion electron Mössbauer spectroscopy at atomic scale

Marek Przybylski

*Solid State Physics Department, Faculty of Physics and Nuclear Techniques,
University of Mining and Metallurgy, al. Mickiewicza 30, 30-059 Kraków, Poland*

The characteristic magnetic phenomena of ultrathin films are attributed to their reduced dimensionality and increased importance of the interfacial properties originated at their boundaries. The loss of nearest neighbor interactions at the interfaces, band hybridization, expansion or contraction of the atomic spacing occur, resulting in local changes of the energy band structure. Recent technical developments make it now possible to grow ultrathin films in a strictly layer-by-layer mode and to produce large areas of flat surfaces. Nevertheless, small structural perturbations in the local atomic configuration can still exist and result in significant changes of the global magnetic properties. Conversion Electron Mössbauer Spectroscopy (CEMS) determines the hyperfine interaction parameters which are sensitive to the arrangement at the atomic scale. In particular, depth selectivity at a monolayer level has been achieved in Fe films with one atomic layer replaced by the Mössbauer isotope ^{57}Fe .

This contribution reviews the experimental work on magnetic phenomena of bcc, fcc and hcp Fe ultrathin films (including monolayer and multilayer structures), epitaxially grown by condensation from molecular beam under ultrahigh vacuum conditions. Since the structural and magnetic information can be achieved by using one method only, Mössbauer spectroscopy is pointed out as being an extremely effective and convenient tool for such purposes.

1. Magnetic properties of ultrathin films, their surfaces, interfaces and multilayer structures

Ultrathin ferromagnetic films, including monolayers, and their multi-structures, have become a subject of considerable attention. This is due to general theoretical interest in low-dimensional magnetic systems and to the progress in calculating their magnetic properties, such as the magnetic moment and magnetic hyperfine fields, by self-consistent methods [1]. The magnetic state of iron atoms depends on their coordination and on the magnetic interaction with their surrounding. Ferromagnetic films in the range of one to several atomic layers exhibit special magnetic properties, connected with their reduced dimensionality, that have a great impact on the general understanding of magnetism. The reduced dimensionality causes a reduction of spontaneous magnetization and the Curie temperature with decreasing the number of atomic lay-

ers [2]. This is due to a simple picture that “strength” of the magnetic interactions has to be dependent on the number of surrounding magnetic atoms. In particular, the temperature dependence of the magnetization $M(T)$ in the thinnest films (its character, dependence on the thickness at finite temperatures, distribution across the films of varied thickness, etc.) remains a subject of serious controversy. Since it is well known that $M(T)$ in three-dimensional ferromagnets is a direct measure of exchange interactions, it is natural to try to take advantage of the spatial resolution of existing experimental methods and to determine, from the local $M(T)$ measured separately in each atomic layer, the character and strength of the local exchange interactions in two (and quasi-two)-dimensional ferromagnets.

The ground state magnetic properties can be modified by the variation of the density of states of the conduction electrons. The Stoner criterion for the existence of ferromagnetism $UD(E_F) > 1$ (where $D(E_F)$ describes the density of states at the Fermi level, U is the exchange energy between two electrons with opposite spins in the same orbital) provides some insight into the differences in magnetic properties that are expected to exist in ultrathin films. The lower atomic coordination associated with atoms in the monolayer films can lead to a reduced overlap of d-electron wave functions and to a related reduction in bandwidth which effects the increase of $D(E_F)$ [1]. Then the reduced overlap and relatively narrow bands can lead to enhanced magnetic moments. In favorable cases, it could even lead to ferromagnetism in monolayer film of metals that are not magnetically ordered in their bulk form. Despite of the large body of theoretical work devoted to the evaluation of the ground-state moment in the dimensionally-reduced magnetic systems, there exist very little experimental data on the absolute value of the magnetic moment in ultrathin films. The main reason of this is that the local measurements of the magnetic moment values are difficult. Secondly, calculations usually refer to the ground-state properties that can be measured at liquid-helium temperatures, and this requirement stays in conflict with *in situ* studies. But, the most important reason is a difference between usually simple model systems chosen for calculations and real systems that can be obtained experimentally. In particular, it should be emphasized that the magnetic properties of a free-standing monolayer is a question of interest, which remains an esoteric question because of the inability to produce such a structure experimentally. It is possible, however, to produce magnetic monolayers supported on a non-magnetic substrate, but then the magnetic behavior is further complicated by monolayer-substrate electronic interactions. In any case, it is well known that in two dimensions only the Ising model describes a spin system, which displays true long range order at finite temperature. In two-dimensional Heisenberg ferromagnets it should not be a long range order, except for systems displaying a large anisotropy. Long wavelength spin fluctuations are strongly excited at finite temperatures and break up the long-range order which is present in the fully aligned ground state. On the other hand, the lack of ferromagnetism at the monolayer level is often attributed to superparamagnetism, which is characteristic for samples with isolated islands. Thermal excitations are then responsible for a random magnetization distribution between each island of the film actually possessing long-range ferromagnetic order.

Stretching (or expanding) the lattice constant in comparison to the bulk by growing strained or expanded layers of the epitaxial film on different substrates can result in drastic changes of the magnetic properties. The recent development in production of epitaxial systems is able to grow strained or expanded layers of different crystallographic symmetry, providing the necessary base to study new phases of materials, like fcc or hcp iron. The latter do not exist as three-dimensional solids under normal conditions, but may be stabilized in the form of a monolayer film on a suitable substrate.

Also the magnetic anisotropy in ultrathin films is strongly modified compared to the bulk material. In a phenomenological approach the competition between surface and shape anisotropy determines the magnetization direction. If the balance between these quantities is changed, a change of the magnetization direction can occur from an orientation in-plane towards perpendicular of the film. This is of great interest because the ability to alter anisotropy values is of technological importance for magnetic recording applications. Fe(110) films provide an example where in addition to the out-of-plane anisotropy mentioned above, in-plane surface anisotropy occurs due to the reduced (2-fold) in-plane local symmetry in this case. A growth induced contribution to surface anisotropy connected with steps as well as coating of Fe films can additionally influence the in-plane surface anisotropy [3,4]. Magnetic surface anisotropy tends to be maximum for free and smooth surfaces and to be reduced by coverage with any solid coating or reaction with gases. This is in accordance with the basic concept of magnetic surface anisotropy as a result of broken symmetry in surfaces [5].

Instead of a single magnetic film on a non-magnetic substrate (which is impractical for technical applications), one can repeat the sequence many times, which means producing a multilayer or superlattice. As a consequence all effects originated from the interfaces and resulting from the reduced dimensionality are multiplied by the number of sequence repetition. Since the discovery of indirect magnetic exchange coupling between two ferromagnets separated by a nonmagnetic interlayer, many sandwich and multilayer structures of this type were investigated experimentally [6]. The coupling was found to be of oscillatory character changing from antiferro- to ferromagnetic depending on the thickness of the nonmagnetic interlayer. The detailed nature and strength of the coupling are supposed to be strongly dependent on the crystallographic orientation, the topology of the Fermi-surface and the local atomic arrangement in the interfaces.

The above mentioned properties form a subject of our basic interests and open some elementary problems remaining to be solved:

- when does a true 2D system (monolayer or submonolayer) become magnetically ordered,
- how does the ordering temperature depend on the number of atomic layers,
- what are the ground-state values of the magnetic moments (or magnetic hyperfine fields) for a monolayer, a double-layer,

- how does the distribution of magnetization across ultrathin film depend on its thickness,
- how does the roughness of interfaces influence an indirect exchange coupling between two ferromagnetic layers, etc.?

The base of our studies is the strong expectation that the magnetic materials can be synthesized in a controlled way and in a form very close to the model systems. Recent technical progress makes it now possible to grow such films “layer-by-layer” and as thin as one monolayer. Due to the application of modern experimental techniques, such as a monolayer resolution conversion electron Mössbauer spectroscopy, the unusual properties of ultrathin films can be studied and analyzed with a spatial resolution on the level of one atomic layer. CEMS has the unique feature of local analysis involving the hyperfine interaction parameters. They are very sensitive to the local modification of the charge and spin densities and their comparison with calculated values allows a very sharp test of the applied theories.

2. Experimental techniques of thin film analysis

To be able to perform an experimental analysis of magnetic phenomena in films consisting of only a few atomic layers, the structure of the films should be well defined and almost perfect. By structure we understand the local microscopic arrangement of atoms as well as the morphology of films on the nanometer scale. Both are expected to be closely connected with magnetic properties. This applies in particular to the thinnest films (monolayer range) where the most important technological problem is how to avoid the formation of islands in the initial stages of growth [7].

Most epitaxial metal films are prepared by evaporation and condensation in ultra-high vacuum. The first attempt to understand the mode of their growth was made by Bauer [8] in terms of classical nucleation theory assuming that the shapes of both the critical nucleus and the overcritical crystallites are determined by the minimum of the surface free energy. The final structures of growing films differ drastically depending on the actual relation between the substrate, interface and film surface free energy. Nevertheless, at equilibrium, layer-by-layer growth can be expected only if the film wets the substrate, i.e., if $\gamma_{\text{substr}} > \gamma_{\text{film}}$. The condition should be fulfilled for each forthcoming atomic layer. The real growth process is determined to a large extent by kinetic principles. Real surfaces exhibit many defects such as steps, adatoms adsorbed from the residual gas even under UHV conditions, vacancies and dislocations, all providing additional nucleation centers. Their influence on the nucleation process is provided by the stronger bonding of atoms due to the increased number of nearest neighbors in adsorption sites and by the disturbances of diffusion controlled processes. The thermal energy of the diffusing atoms can be influenced by the experimentalist *via* the substrate temperature. It is general experience [9] that a layer growth can be induced either by a high evaporation rate or a reduced growth temperature even in nonwetting systems. Epitaxial growth of the films is then a result of a delicate balance

between layer growth forcing by supersaturation (which requires low temperatures) and good crystalline order (which requires high temperatures).

Another parameter which determines the structure of epitaxially grown film is the lattice misfit of the film to the substrate ($f = (a_f - a_s)/a_s$, where a_f and a_s are the lattice parameter of the film and the substrate, respectively) which can be accommodated by elastic strain or by misfit dislocations. For small misfits, it may be energetically favorable to accommodate completely to the substrate by elastic strain without any dislocations, forming a pseudomorphic film in which all atoms occupy substrate-atoms positions in the plane. The elastic energy of a pseudomorphic monolayer is proportional to f^2 , whereas the dislocation energy of the misfitting monolayer depends on the density of dislocations which is proportional to f . Therefore there is a critical misfit, being of the order of 10% depending on the elastic properties of film and substrate, below which the monolayer is pseudomorphic. Film remains pseudomorphic up to the critical thickness, which is as a rule the larger it is the smaller is the misfit. Above the critical thickness, misfit dislocations help to accommodate the misfit. The most important question is up to what thickness the films grow pseudomorphically? The further question is whether the first atomic layer (or layers), which are pseudomorphic during the growth, remain pseudomorphic in the interface of the thicker film. In addition, the strain energy contributes to the surface energy of the film. As a result, if the strain energy becomes large it could be energetically preferable to form three-dimensional islands on top of the initially continuous film.

Finally, the preparation of metallic film systems is restricted by interdiffusion and alloying between substrate and film atoms as well as between film and its coating. An ideal case occurs if interdiffusion is forbidden by the phase diagram.

If a complete analysis of the local magnetic properties of surfaces, interfaces and ultrathin films is desired, selection of the investigated system (substrate-film-coating) as well as the choice of the applicable experimental techniques are of prime importance. The optimal solution seems to be the combination:

- (i) of a proper substrate–film system and proper preparation conditions, in order to attain layer growth of monocrystalline films or any special structure of the film which is required,
- (ii) of proper ultra-high vacuum conditions of preparation to assure atomic purity of the films and surfaces,
- (iii) of suitable techniques for structural and chemical analysis of films and surfaces (e.g., AES (Auger Electron Spectroscopy), LEED (Low Energy Electron Diffraction), RHEED (Reflection High Energy Electron Diffraction) and STM (Scanning Tunneling Microscopy)) applied *in situ* (these should adequately specify the structure of films as well as their mode of growth),
- (iv) and of a suitable experiment for local analysis of the magnetic quantity to be directly compared with its value calculated theoretically.

In principle, a lot of experimental techniques are applicable for probing the magnetic state of ultrathin films and surfaces, such as Spin Polarized Photoemission [10], Surface Magneto-Optic Kerr Effect [11], Torsion Oscillation Magnetometry [12]. However, as they essentially yield only integral information or can be applied only to free surfaces, local analysis of the magnetic properties and their variations is not possible. In particular, local analysis of magnetic order cannot be performed using magnetometry which has no layer-by-layer resolution. Therefore, the spatial distribution of magnetic moment, μ , which is a basic magnetic quantity, cannot be experimentally measured.

The magnetic hyperfine field can be measured by PAC (Perturbed Angular Correlations) [13], NMR (Nuclear Magnetic Resonance) [14] and Mössbauer effect [15,16]. PAC is very suitable for accurate measurements of the nuclear electric-quadrupole interactions. Its sensitivity is independent of temperature. NMR is particularly useful for measuring of chemical shifts. Mössbauer effect can be used to measure both chemical shift and electric-quadrupole interaction, and nuclear magnetic hyperfine fields as well. However, Mössbauer measurements are only possible on crystals that contain a Mössbauer isotopes and the spectral intensity depends on temperature. Each of these techniques requires a different number of nuclear probes. NMR requires 10^{15} probe atoms, therefore is specially dedicated to the multilayers. Mössbauer spectroscopy requires approximately 10^{13} probe atoms in the case of “absorber experiment” (and much below 10^{13} in the case of “source experiment”) which amount is sufficient to achieve sub-monolayer sensitivity. PAC requires only about 10^{11} – 10^{12} probe atoms and therefore it is particularly useful to study the very local morphology of the surfaces [17].

2.1. Conversion electron Mössbauer spectroscopy

The Mössbauer effect has provided the most efficient contribution to ferromagnetism and to that of thin films in particular. The unique advantage of this technique, compared with other methods, is connected with its isotopic character: using ^{57}Fe atoms as probes, local analysis of magnetic hyperfine field can be achieved [18]. In this context, the local character of Mössbauer spectroscopy is of great advantage, for the following reasons:

- (i) in a film consisting of a few atomic layers of ^{56}Fe , it is possible to replace exactly one monolayer by the Mössbauer isotope ^{57}Fe ; then the measured spectrum is a strictly local analysis of the hyperfine interaction parameters [18]; one of them, the magnetic hyperfine field, B_{hf} , becomes a local probe of magnetic order,
- (ii) even in a film consisting of pure ^{57}Fe , local analysis is possible if the magnetic hyperfine field varies markedly from one atomic layer to another [16].

In order to measure Mössbauer spectra with a sub-monolayer detection sensitivity achievable in reasonable time, conversion electron Mössbauer spectroscopy is required to be applied. In comparison with the transmission technique, Mössbauer spectroscopy of conversion electrons (CEMS) shows several advantages:

- (i) limitation of minimum absorber thickness is no longer obligatory due to the much lower detection limit of CEMS, moreover internal conversion is much more probable than emission of γ -radiation,
- (ii) on the other hand, CEMS in backscatter mode can be applied to surfaces of bulk specimens, just like emission Mössbauer spectroscopy if the sample is prepared as a Mössbauer source; however, the need to handle a radioactive isotope in emission Mössbauer spectroscopy restricts the applicability of the method in this case,
- (iii) handling electrons, such as filtering their energy to improve the signal-to-noise ratio, is technically straightforward.

Application of the CEMS method to the analysis of thin films (and surfaces) demands compliance with a number of requirements [19,20]. An essential problem to be solved is how to improve the signal-to-noise ratio and the detection limit of the CEMS method. It is important to achieve sub-monolayer sensitivity within the limit of few hours per one ^{57}Fe monolayer spectrum to be measured. Both the detection limit and the signal-to-noise ratio are determined by the relationship between the number of electrons emitted in resonance (conversion and Auger electrons) and by the number of electrons emitted out of resonance (background). Electrons from numerous sources contribute to non-resonant background, decreasing this ratio. The most important are photoelectrons emerging from all the surrounding elements being irradiated by gamma-quanta. Iron itself increases non-resonant background with Fe-7.3 keV-photoelectrons, because their energy and the energy of conversion electrons are the same and cannot be energetically filtered. The 7.3 keV-photoelectron contribution to the background is small due to the value of its cross-section (which is two orders of magnitude smaller than that for Mössbauer absorption), but the number of photoelectrons depends on the total film thickness (whereas the conversion electrons originate principally from one atomic layer of ^{57}Fe only). Another disadvantage of thicker films is that they require more material increasing the amount of contamination being proportional to the film volume. On the other hand, thick enough films can simulate a semi-infinite sample (and its surface) and all structural imperfections resulting from a lattice mismatch between the film and the substrate are lost. Therefore, a total thickness which is chosen for surface study, is a compromise with respect to all the above considerations.

Conversion electron Mössbauer spectroscopy of thin films and their surfaces can be realized in three ways:

- (i) as integral CEMS which involves the detection of all emerging electrons, regardless of their energy,
- (ii) as depth-selective CEMS, i.e., by performing an analysis of the energy of conversion electrons; the energy loss of conversion (and Auger) electrons clearly correlates with the depth at which they originate [22],
- (iii) as ^{57}Fe probe monolayer CEMS, which is actually integral CEMS, but all electrons emerge from one atomic layer only; only this layer consists of ^{57}Fe atoms, while

the remaining material is ^{56}Fe ; therefore integral CEMS now features depth-selectivity, moreover, at atomic layer level.

The first method is usually applied to follow the global parameters of the film as a whole. For such studies thin films are usually prepared from pure ^{57}Fe , thus the method is called pure ^{57}Fe film analysis. Note, that even in a film consisting of N atomic layers of pure ^{57}Fe , local analysis is possible if the magnetic hyperfine field varies markedly from one atomic layer to another (N sets of hyperfine parameters are available) [16].

The second method has not been included in the present discussion because of its insufficient depth resolution, definitely worse than the monolayer level [22,23].

The third method is applied in order to follow layer-by-layer distribution of hyperfine parameters. Monolayer sensitivity of the method is assured by filtering and efficient detection of the emitted electrons. Monolayer resolution is obtained by preparing exactly one monolayer of ^{57}Fe placed at a chosen distance from the surfaces/interfaces (figure 1) [24]. The hyperfine parameters are profiled by varying the position of the ^{57}Fe probe monolayer. The reliability of the ^{57}Fe atom distribution in one atomic layer only is assured by the exquisite method of film preparation. If a single monolayer of ^{57}Fe is used as the local probe of hyperfine interactions, the method is called probe ^{57}Fe monolayer analysis.

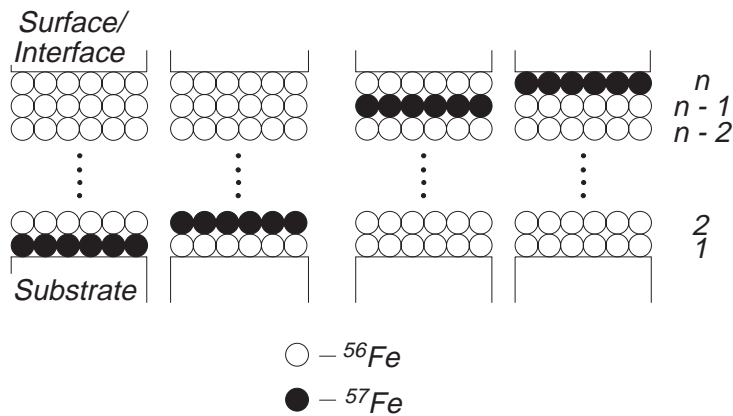


Figure 1. Schematic representation of the probe ^{57}Fe monolayer conversion electron Mössbauer spectroscopy. Exactly one monolayer of ^{57}Fe is prepared and placed at the chosen distance from the surface.

Mössbauer spectra are expected to reflect the layer structure of the films as well as their structural imperfections. This is due to the direct correlation between the actual structure and the local magnetic properties of the films which is reflected in the appropriate components of the spectra and in their parameters, e.g., in the magnetic hyperfine field. The measured effective hyperfine field, B_{hf} , in zero applied external magnetic field may be decomposed into four contributions:

$$B_{\text{hf,eff}} = B_{\text{hf,cp}} + B_{\text{hf,ce}} + B_{\text{hf,orb}} + B_{\text{hf,dip}}.$$

$B_{\text{hf,cp}}$ is the Fermi contact field from polarization of the core s-electrons, which should be proportional to the local Fe magnetic moment. $B_{\text{hf,ce}}$ is the field transferred to the ^{57}Fe nucleus by the conduction electron spins polarized via the RKKY interaction. This term represents a non-localized contribution which depends on the local environment and can, therefore, be different at the surface, in the ultra-thin film and in the bulk. $B_{\text{hf,orb}}$ is the dipolar contribution from the orbital magnetic moment. $B_{\text{hf,orb}}$ vanishes for bulk metallic Fe and its cubic alloys. $B_{\text{hf,dip}}$ is the sum of dipolar fields from the spin magnetic moments. The summation is usually broken down into on-site and off-site contributions. The on-site contribution is small in metallic Fe due to the spherical symmetry of the orbital with $L = 0$. The off-site contribution includes the demagnetizing field $B_{\text{hf,d}}$ and the Lorentz field $B_{\text{hf,L}}$. In an infinitely large, perfectly smooth thin plate with the magnetization parallel to the plane $B_{\text{hf,d}} = 0$. $B_{\text{hf,L}} = M/3$ for cubic symmetry, where M denotes magnetization. At the boundary of a ferromagnet, however, $B_{\text{hf,L}}$ is not defined and the on-site contribution to $B_{\text{hf,dip}}$ does not vanish. If the surface is not perfectly smooth, local demagnetizing fields, $B_{\text{hf,d}}$, which increase with the surface roughness are also expected to occur in the film. Decomposition into $B_{\text{hf,d}}$ and $B_{\text{hf,L}}$ fails for surfaces. The relative intensities $I_{i,j}$ of the six line Zeeman spectrum for the magnetic interaction are connected with the angle α between the direction of magnetization and the incident γ -ray by:

$$I_{1,6} = 3(1 + \cos^2 \alpha), \quad I_{2,5} = 4 \sin^2 \alpha, \quad I_{3,4} = 1 + \cos^2 \alpha.$$

Detailed understanding of magnetic properties of ultrathin films requires a detailed knowledge of the film structure at the atomic scale. Since the structural and magnetic information can be available in a local way and also achieved by using one method only, conversion electron Mössbauer spectroscopy appears to be an extremely effective and convenient tool for the purpose being illustrated with the following examples of bcc-, fcc- and hcp-Fe films.

3. bcc-Fe films on W(1 1 0) (including monolayer)

Ferromagnetic order in a two-dimensional lattice is one of the most fascinating subjects in the field of thin film magnetism. Due to a preparation dependent three-dimensional growth of Fe on different substrates, experimentally found properties of two-dimensional ferromagnets were never clearly related to the well documented two-dimensional distribution of the atoms. Ferromagnetic order in two dimensions was detected for the first time for an Fe monolayer on W(1 1 0), which displays strong in-plane magnetic anisotropy which is supposed to trigger the long-range magnetic order [7,25,26]. The problem of the existence of two-dimensional translational symmetry was solved by pseudomorphic growth of a monolayer on a matching substrate. The structural interpretation of the spectral components, with the aim of proving a unique correlation between the atom positions and the corresponding components of the discussed spectra, is based first of all on the presence or absence of components related to the sample thickness. Therefore, the component only existing in the spectra of the

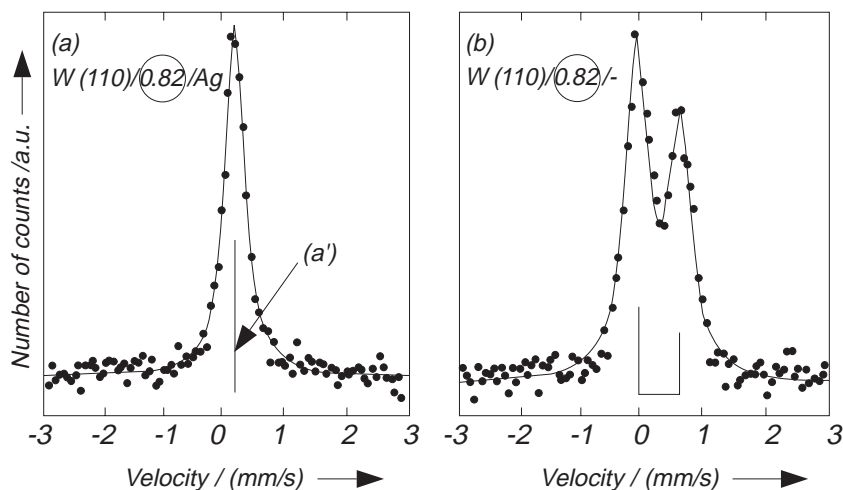


Figure 2. Room temperature Mössbauer spectra of a monolayer of Fe(110) on W(110), coated with Ag and uncoated, (a) and (b), respectively (taken from [23]). $D = 0.82$ of bulk monolayer corresponds to the coverage $\Theta = 1$, i.e., to a completed pseudomorphic monolayer.

thinnest Fe films on W(110) (figure 2(a) and (b)) is supposed to be due to monolayer patches. An asymmetric quadrupole doublet is observed for the uncoated monolayer (figure 2(b)) rather than the single line for the coated one (figure 2(a)). This reflects the lower symmetry of surface atoms in comparison with interface atoms, in qualitative agreement with results for the surface and interface of a semi-infinite Fe film. The doublet asymmetry is due to the angle of 75° between the direction of γ -quanta propagation and the direction of the main axis of the EFG tensor (perpendicular to the film plane) resulting from the experimental geometry.

For coverage below monolayer, the CEMS spectra consisted uniquely of the monolayer components. They show a transition from the paramagnetic to the ferromagnetic state at a temperature slightly reduced below room temperature. Because the CEMS measurement time is long for such a submonolayer coverage, detailed analysis was performed for the films coated with Ag to avoid residual gas adsorption. The most important result is that at 90 K a Zeeman sextet with $B_{\text{hf}} = 11$ T was detected for all the films of the coverage $0.4 < \Theta < 1$ of completed atomic layers, independently of the coverage and temperature of preparation. The temperature dependence of B_{hf} for the complete monolayer prepared at 475 K is shown in figure 3. For the uncoated films the measured value of B_{hf} is reduced to about 10 T. The films prepared at room and elevated temperature become ferromagnetic above the coverage of $\Theta = 0.60$ and $\Theta = 0.11$, respectively.

It is evident that a film thicker than one monolayer should contain monolayer and double-layer patches. The microscopic, local character of CEMS allows us to see them separately. Room temperature Mössbauer spectra for $\Theta > 1$ (figure 4) consist of a single-line component (a) in the central part of the spectra and of two additional mag-

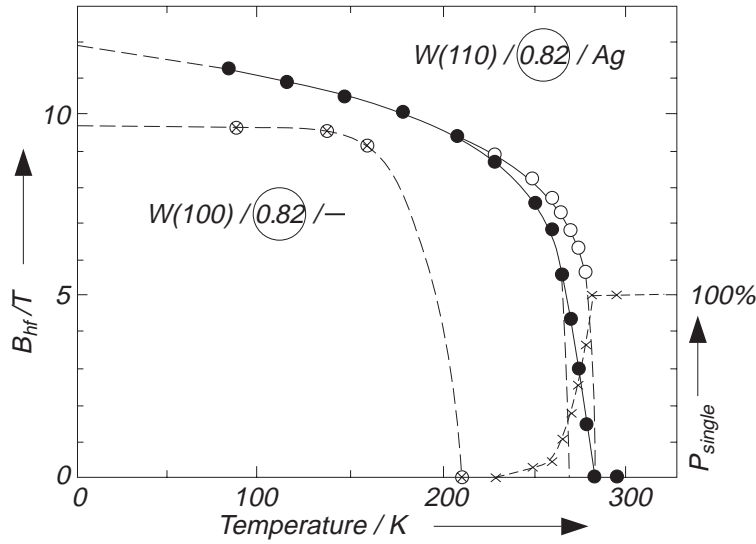


Figure 3. Magnetic hyperfine field B_{hf} of the magnetic component (\circ), mean magnetic hyperfine field (\bullet) and single line contribution $p_{\text{single}}(x)$ vs. temperature, for a pseudomorphic monolayer of Fe(110) ($\Theta = 1$) on W(110) prepared at 475 K. The values for uncoated monolayer (\otimes), obtained by extrapolation to time just after preparation (b), are included. T_c for the uncoated monolayer is obtained from thermal scan (taken from [25]).

netic components (b) and (c). Components (b), $B_{\text{hf}} = 18$ T, and (c), $B_{\text{hf}} = 28$ T, appear in films only slightly thicker than one monolayer, their intensity increases with increasing thickness. Therefore, a simple interpretation, namely that these two components belong to the W and Ag side of the double-layer patches, was proposed. The intensities of both components are not exactly the same, which is probably due to slightly different values of the recoilless fraction factor, f , in both layers. At low temperatures the monolayer component reflects a transition from the para- to the ferromagnetic state. The value of B_{hf} at 90 K is exactly the same as for the thermodynamically stable monolayer. No qualitative differences between spectra of coated and uncoated films of the same thickness were observed, except for the case of the monolayer discussed above. This is clearly seen in CEMS-spectrum of an uncovered film of $\Theta = 1.3$ measured at 150 K (figure 5). Despite of the broad lines connected with an adsorption of the rest gases existing in UHV-chamber, the spectrum can be again fitted by a superposition of three magnetic sextets with $B_{\text{hf}} = 10.5$ T (corresponding to the monolayer), $B_{\text{hf}} = 18.2$ T and $B_{\text{hf}} = 31$ T (corresponding to double-layer patches) and of their relative contributions $p_1 = 54\%$, $p_2 = p_3 = 23\%$, respectively. The coverage calculated from the relative contributions $\Theta = 1.34$ remains in excellent agreement with the value measured with the quartz balance ($\Theta = 1.3$) [21,27]. The newest results concerning the system are even more exciting. In a range of coverage between $\Theta = 1.20$ and $\Theta = 1.48$ atomic layers, in the films prepared at 300 K, long range ferromagnetic order (detected magnetometrically in the film plane) is suppressed [28]. It means that

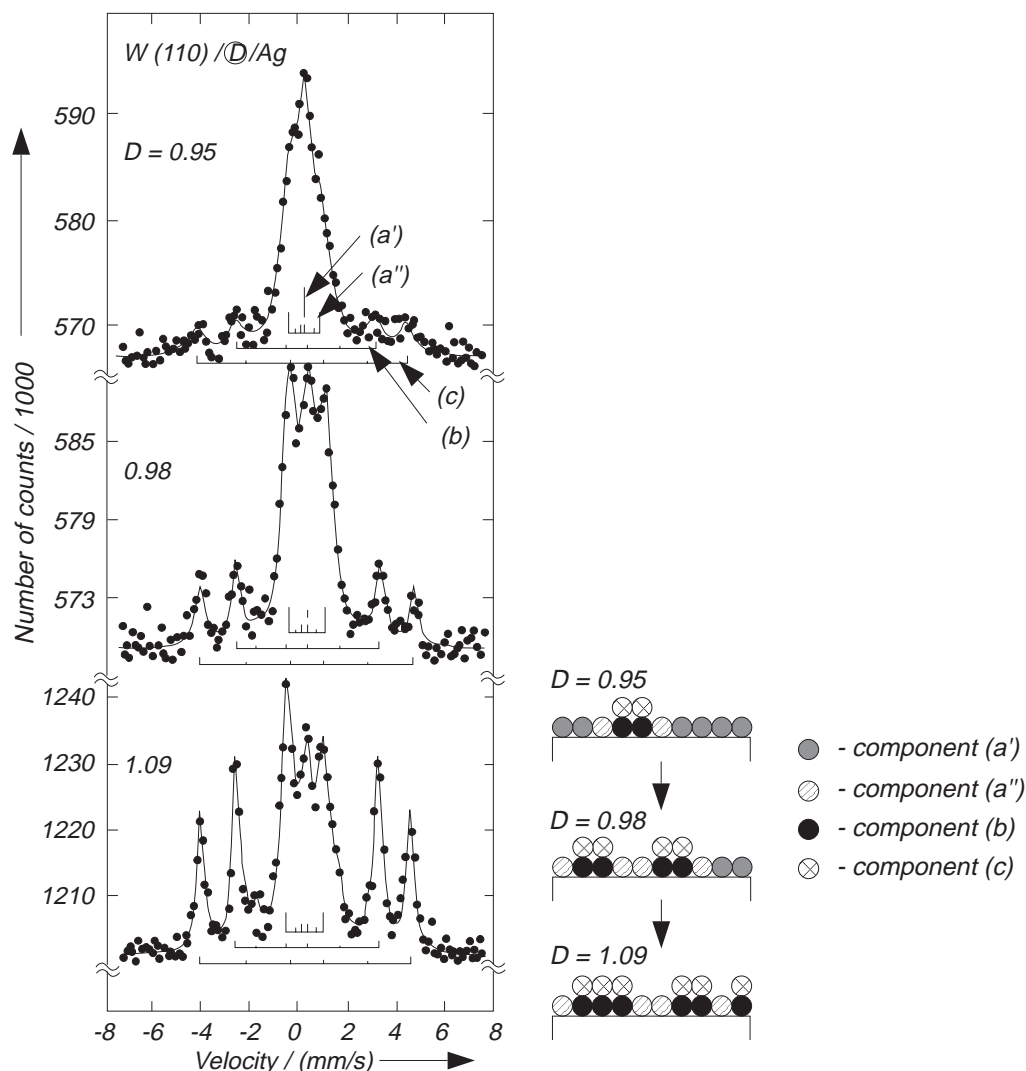


Figure 4. Room temperature Mössbauer spectra of the $^{57}\text{Fe}(110)$ films of the thickness just above a monolayer, prepared on $\text{W}(110)$ and coated with Ag at room temperature (taken from [21]).

both the double layer islands and the monolayer region in between are statistically magnetized up and down along the easy axis (i.e., that some kind of antiferromagnetic order exists). Another possibility is that the double-layer patches are magnetized out of the film plane, i.e., perpendicular to the direction in which the magnetization measurements were performed. Unfortunately, due to the actual geometry of CEMS measurements and relatively poor quality of the spectra (measured at low temperature for uncovered film) we were unable to distinguish between these possibilities. The fact that the Mössbauer spectrum measured at 150 K consists of three “magnetic” sextets does not contradict the lack in ferromagnetic order observed in a macroscale

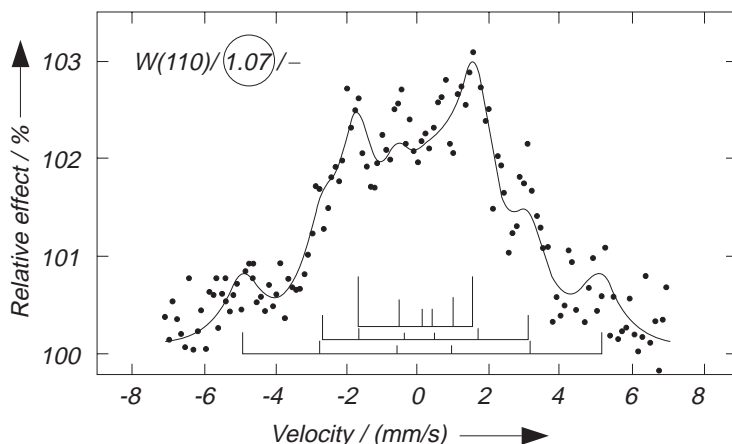


Figure 5. Mössbauer spectrum of uncoated Fe(110) film of thickness just above a monolayer measured at 150 K (taken from [27]).

of the film but it relates to the sensitivity of Mössbauer spectra to the local magnetic hyperfine field. Just recently Gradmann et al. [29] reported that magnetic anisotropy of the system is actually uniaxial, but the easy axis switches between out-of-plane for the double-layer islands and in-plane for the monolayer surrounding. The monolayer regions remain ferromagnetic and magnetized in-plane, however strongly influenced by ferromagnetic coupling between the double-layer patches. Perpendicular magnetization of the double-layer patches is induced by mechanical stresses existing due to the large lattice mismatch between Fe and W(110) (about 10%). In accordance to a general rule that magnetic surface anisotropy tends to be reduced by coverage with any reaction with gases, the easy axis switches to in-plane after an exposure of about 1–2 Langmuir. It corresponds to 2–3 hours of deposition even if vacuum is of the order of 10^{-10} mbar. This is why the Mössbauer spectra, measured 24 hours, were unable to detect the out-of-plane magnetization found only just after preparation.

An Fe monolayer on W(110) (as well as monolayer patches) is thermodynamically very stable. We found no experimental evidence of reconstruction of Ag-coated and uncoated films consisting of Fe atoms in the first atomic layer on W(110), at temperatures up to 875 K. This is opposite, e.g., to the Cu-covered films which undergo considerable structural changes and the relative contributions of the spectral components do not follow layer-by-layer growth predictions, even if coating is carried out at room temperature [30]. Annealing of such a film leads to a completely changed spectrum, 90% of which consists of a single line which remains dominant even in the spectrum measured at 90 K. This can be confronted with the results for monolayer of Fe(110) coated by Cu at strongly reduced temperature (90 K) and measured directly after that. Then the obtained spectrum consists of one Zeeman sextet with $B_{\text{hf}} = 10.8$ T. One can conclude that at room temperature and above Fe dissolves in Cu, probably forming superparamagnetic clusters. This phenomenon correlates with

the relatively high surface energy of Cu ($\gamma_{\text{Cu}} = 1.7 \text{ J m}^{-2}$), compared with that of Ag ($\gamma_{\text{Ag}} = 1.1 \text{ J m}^{-2}$) [31].

3.1. Temperature dependence of magnetic order

It is commonly accepted that at finite temperatures the film magnetization decreases with reduction of film thickness. In frame of the spin-waves theory, in the range of ultrathin films and at low temperatures, spin-waves with $k_z \neq 0$ are not excited and the number of magnons, n_m , is independent of film thickness. The total magnetic moment of the film, μ , is then proportional to the film volume, V , which is given as the interlayer spacing, A , multiplied by the number of actual atomic layers:

$$\mu = M_0 V - 2\mu_B n_m = M_0 \Theta A S - 2\mu_B n_m,$$

where M_0 denotes the bulk magnetization and S denotes the area of the film. The deviation of magnetization at finite temperature is given by:

$$\Delta M = M_0 - M = M_0 - \mu/V = 2\mu_B n_m / (AS\Theta),$$

and is proportional to the reciprocal of the number of atomic layers Θ . Thus, the much stronger dependence of magnetization on temperature for one atomic layer in comparison with the bulk, can be easily understood. The $T^{3/2}$ -law is appropriate for a phenomenological description of the temperature dependence of the average magnetization (and B_{hf}). The spin-wave parameter b can be used to describe the dependence of average magnetization on thickness at a finite temperature. Such dependence of b on the reciprocal of the number of actual atomic layers of Fe(1 1 0) on W(1 1 0) is presented in figure 6. Data for Fe films sandwiched between Cr(1 1 0) and Ru(000 1) are included for comparison. An average value of b for Fe(1 1 0) films sandwiched between the Cr-matrix, in comparison with our model system of Fe(1 1 0) between non-magnetic W and Ag, is smaller in a whole thickness range including the thinnest

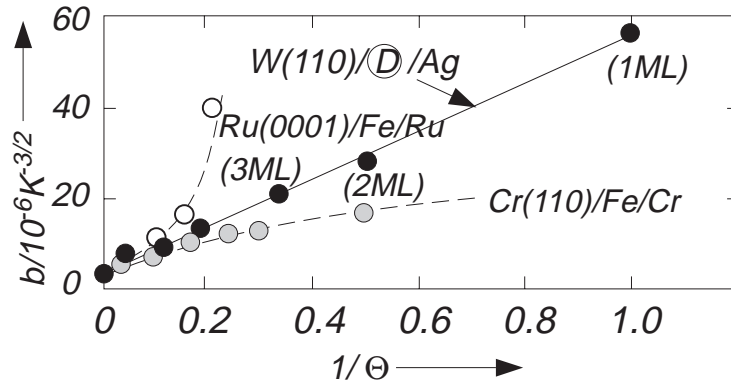


Figure 6. Average spin wave parameter b as a function of the reciprocal of the number of actual atomic layers, Θ , of Fe(1 1 0) on W(1 1 0), Fe(1 1 0) sandwiched between Cr and Fe sandwiched between Ru (data for W/Fe/Ag taken from [34], data for Cr/Fe/Cr taken from [45], data for Ru/Fe/Ru taken from [58]).

films. It confirms that exchange interactions are continued through interfaces into the interfacing Cr magnetic films resulting in weakened magnetic size effect. The high values of b for the thinnest Fe films sandwiched between Ru(0001) matrix are caused by a discontinuity in the layer structure of the films and resulting superparamagnetic effect [32].

3.2. Curie temperature

Modification of spin dynamics at finite temperatures in films consisting of a few atomic layers results in a decrease of Curie temperature (T_c) with decreasing number of layers [33]. In agreement with simple mean-field arguments, T_c should be proportional to the number of the nearest neighbors. At the initial stages of film growth, the Curie temperature is a local quantity which depends on the number of atomic layers in the patches that form the film and have a different number of the magnetic neighbors. In particular, in the case of an Fe(110) monolayer, the number of the nearest neighbors is reduced from $z_1 = 8$ (for bulk Fe) to $z_1 = 4$. Therefore for a thermodynamically stable monolayer (or monolayer patches large enough to represent a true monolayer) we expect a well defined but strongly reduced value of T_c in comparison with that of bulk Fe. The Curie temperature of small monolayer patches could be increased a little above the monolayer- T_c due to an interaction with the neighboring double-layer patches (for $\Theta > 1$) or decreased due to the finite diameter of the patches (for $\Theta < 1$). One can imagine that the Curie temperature depends on the diameter of the monolayer patches in a similar way as it depends on the thickness. Consequently, a decrease of T_c for the small monolayer patches consisting of a limited number of atoms surrounded with a limited number of magnetic neighbors is expected. Using CEMS, the Curie temperature can be measured relatively easily by the thermal scan method and is then defined as the temperature at which the line width of the measured single line (above T_c) approaches the instrumental value (number of counts at a corresponding fixed source velocity saturates). Otherwise, if T_c is estimated from the temperature dependence of B_{hf} as the temperature at which $B_{hf} = 0$, one must solve the issue of extrapolating B_{hf} values in the critical region. Using the thermal scan method [34], T_c was determined for Ag-coated films, under different preparation conditions. The most important result is the constant value of $T_c(\Theta = 1) = 282$ K for $0.4 < \Theta < 1$, if films are prepared at an elevated temperature of $T_p = 475$ K, or annealed up to $T = 875$ K after preparation at room temperature [7,23]. This means that recrystallization to a large monolayer takes place for these conditions. Despite of the large lattice mismatch between W(110) and Fe(110) the monolayer remains continuous and pseudomorphic independently of preparation (or annealing) temperature. Some additional arguments for the high stability of the first atomic layer on W(110), resulting in its dislocation-free perfect pseudomorphism, come from the film strain analysis [35]. The stress measurements show some kind of compressive surface stress existing on the surface of W(110) which leads to zero stress of the system just for the completed monolayer. Then the stress increases linearly with the increasing coverage changing the slope at

approximately 1.5 ML, just at the thickness where the beginning of the formation of misfit dislocations is observed by STM [36].

On the other hand, for samples prepared at $T_p = 300$ K, T_c strongly depends on Θ . This indicates fine-grained substructure of the film. The monolayer patches are too small to be considered as microscopic monolayer. For the films thicker than monolayer, complicated coupling phenomena indicating both weakly magnetic monolayer patches and strongly magnetic double-layer patches must be considered as responsible for an increase of T_c . For an uncoated monolayer prepared at an elevated temperature, the value of $T_c(\Theta = 1) = 210$ K is a rough one due to experimental complications connected with adsorption of residual gases even at 3×10^{-10} mbar. The idea that the Curie temperature is connected with the number z_1 of magnetic nearest neighbor atoms is clearly confirmed by a comparison between the values of T_c for the monolayer of Fe(110) on W(110) and for the double-layer of Fe(100) on W(100). For the double-layer Fe/W(100) the number of nearest Fe-neighbors for Fe atoms in both atomic layers is $z_1 = 4$, exactly the same as for the monolayer Fe/W(110), resulted in the same value of $T_c = 220 + 10$ K. The same applies for Fe films on W(100) and W(110) coated with Ag, however, with a little higher Curie-temperature T_c of approximately 280 K [37].

The model of “monolayer formation” (suggested above *via* a dependence of the Curie temperature on the coverage) was recently confirmed using Scanning Tunneling Microscopy (STM) and related to the onset of the magnetic order that has been studied with CEMS and Spin Polarized Low Energy Electron Diffraction (SPLEED) [38]. Note, that both STM and SPLEED can be applied to uncovered films. In contrast, detailed CEMS measurements in submonolayer regime were applied only for the Ag-covered Fe films. The local atomic arrangement in this case was deduced indirectly from magnetic properties of the films. Therefore, what was expected for an Ag-covered film is now compared with an uncovered one. What do we see in STM images? First of all, the growth is qualitatively different at different temperatures of preparation, as expected. For preparation at elevated temperature a step flow growth is observed from the steps of the substrate. The second layer starts to grow only after completion of the first one. Thus the magnetic behavior is reasonable: T_c depends only slightly on coverage and increases monotonously approaching (already around $\Theta = 0.3$ ML) the temperature of 230 K, which is taken as the Curie temperature of the uncoated monolayer, in good agreement with our previous estimates [7]. For preparation at room temperature growth starts by islands, as expected. The islands remain separated by channels for coverage below 60% of the substrate area, above this coverage coalescence starts between the islands. The magnetic properties of the films confirm the strong dependence of the Curie temperature on the thickness, suggested for Ag-covered submonolayers from CEMS analysis, but only for coverage above 60% ($\Theta = 0.60$ ML)! Below, at least at 115 K (the lowest possible temperature of SPLEED measurements at Clausthal), the films are nonmagnetic; probably they consist of small separated islands which are superparamagnetic. This is not contradictory to the results for the Ag-covered monolayer: the thinnest film we have measured was still

below the limit for Ag-covered island areas for which the superparamagnetic transition occurs at 115 K. The most exciting phenomenon is the steep rise in a narrow coverage interval of only 2% from a completely nonmagnetic state to a magnetic state at 60% of coverage. It means that magnetic percolation takes place near or just before structural coalescence [38].

3.3. Ground-state magnetic properties

It is reasonable that a lower coordination has obvious consequences for the electronic band structure and for the resulting values of $B_{\text{hf}}(0)$. For a system of lower dimensionality the wave functions become more atomic-like. As usual, in the case of 3d-metals, the 3d-band becomes narrower and the states are more localized than bulk ones. Theoretical calculations are always coherent with this simple picture and, consequently, the magnetic moment is a monotonic function of the dimensionality. Therefore a free standing monolayer is expected to exhibit even stronger magnetic enhancement than the surface layer because of its more reduced atomic coordination number. But our Fe monolayer, instead of being a free-standing one, is supported on tungsten substrate which influences the electronic band structure by hybridization between d-bands.

Experimentally, the temperature dependence of B_{hf} for monolayer patches, true monolayer and for the coverage below monolayer of Fe on W(1 1 0), at low temperature limit, shows that this is a general feature, independent of Θ , and in general independent of temperature of preparation. Taking into account all arguments concerning the accuracy of the $B_{\text{hf}}(T)$ fit, $B_{\text{hf}}(0) = 11.9 \pm 0.3$ T was taken as a reliable result for the ground-state value of the magnetic hyperfine field for a true monolayer [39]. Some experiments were performed on an uncoated monolayer [39], where residual gas adsorption interferes, even at UHV conditions. Separate preparations had to be made for each temperature of measurement, and $B_{\text{hf}}(T)$ had to be determined by extrapolation to the time just after preparation. Therefore only a rough estimate of $B_{\text{hf}}(0) = 10 \pm 1$ T was possible for the uncoated monolayer.

Band-structure calculations for the Fe(1 1 0)-monolayer system on W(1 1 0) had been performed by Freeman's group a few years ago [40]. The highly precise self-consistent all-electrons full-potential linearized-augmented-plane-wave method (FLAPW) based on the local spin density approximation, including a calculation of interlayer relaxations by total energy minimization, was applied. To investigate the properties of uncovered and Ag-covered Fe monolayers on W(1 1 0), the system was approximated as a single slab consisting of five layers of W(1 1 0) covered with one monolayer of Fe (and Ag for the Ag-covered case) on each side. The calculated Fermi-contact hyperfine fields ($B_{\text{hf},c}$) are decomposed into core- ($B_{\text{hf},cp}$) and conduction- ($B_{\text{hf},ce}$) electron contributions. The core electrons contribute to $B_{\text{hf},c}$ with a large negative value, which scales exactly with the magnetic moment. The conduction electrons contribute to $B_{\text{hf},c}$ with a positive value, due to direct polarization, and greatly reduce the magnitude of the total Fermi-contact term. Note that the contribution from 4s conduction

electrons is strongly dependent on the environment of Fe atoms. Consequently, this contribution for the monolayer is more atomic-like than that at the surface of clean Fe(1 1 0) due to the larger Fe–Fe atomic distance (the Fe monolayer is pseudomorphic with the W-substrate) and, on the other hand, because 4s electrons do not participate in Fe–W hybridization. Covering with Ag results in an enhancement of the magnitude of the total contact hyperfine field. The amount of enhancement (2.9 T) is very consistent with the CEMS experimental value (1.9 T), obtained as a difference between B_{hf} measured for Ag-coated and uncoated monolayers, respectively. However, for absolute values, only when the unquenched orbital-angular-momentum (+4.4 T) and dipolar contributions (+1.1 or –0.3 T, depending on the spin direction) are included, the total hyperfine field values reduce to those measured experimentally [23,25]. Considering the various approximations made in the calculations, agreement is remarkably good: $B_{\text{hf}}(0)$ is equal to 9.3 and 10.7 T, compared with the experimental values of 10 and 11.9 T, for the uncoated and the Ag-coated monolayer, respectively.

The ground-state value of B_{hf} in the first Fe monolayer on W(1 1 0), if coated with further Fe, is independent of thickness and equals $21.5 + 0.5$ T, strongly reduced in comparison with 33.9 T in the bulk [16,41,42]. This must be interpreted basically as a result of electronic d–d interaction in the W/Fe interface. Unfortunately, band structure calculations for the Fe/W interface of thick Fe films are not yet available. It can be stated only roughly that Fe-3d and W-5d hybridization causes a reduction of the Fe magnetic moment and results in a decrease of the contact magnetic hyperfine field, as compared with FLAPW calculations for Fe monolayer on W(1 1 0). Some insight to the problem comes from the comparison with diluted Fe–W (1–9 at% W) alloys and corresponding Mössbauer data. The reduction of B_{hf} at a given Fe-nucleus, induced by z_1 nearest and z_2 next-nearest W neighbors, is given by $\Delta B_{\text{hf}}(z_1, z_2) = (-4.1z_1 - 2.6z_2)$ T. For an Fe atom at the bcc(1 1 0) interface, $z_1 = 2$ and $z_2 = 2$, resulting in $\Delta B_{\text{hf}}(2, 2) = -13.4$ T, in good agreement with our experimental finding of $\Delta B_{\text{hf}}(2, 2) = -12.5$ T. The same applies for an Fe atom at the bcc(1 0 0) interface with W(1 0 0) (note a different surface with the atoms of a different number of nearest and next-nearest neighbors, $z_1 = 4$ and $z_2 = 1$) resulting in $\Delta B_{\text{hf}}(4, 1) = -19$ T. In the second atomic layer of Fe on W(1 0 0) $z_1 = 0$ and $z_2 = 1$, resulting in $\Delta B_{\text{hf}}(0, 1) = -2.6$ T. The experimental findings of $\Delta B_{\text{hf}}(4, 1) = -20.7$ T (in a first layer of Fe(1 0 0) on W(1 0 0)) and $\Delta B_{\text{hf}}(0, 1) = -4.4$ T (in a second layer of Fe(1 0 0) on W(1 0 0)) remain in remarkable agreement at least for the first monolayer. This encourages discussion of magnetic interface phenomena in comparison with the corresponding alloys. Usually, comparison between the interfaces and disordered alloys is provided in the opposite direction. At first, the magnetic hyperfine field B_{hf} for the certain coordination corresponding to the actual atomic coordination in the ideal interface (characterized by the same number of nearest neighbors) is extracted from an alloy spectrum. Then the interface-spectrum component found as being of the same B_{hf} is attributed to the interface. The intensity of the component is taken as a measure for the population of Fe atoms sitting at a position of the sharp interface. For example, an effect of Cr nearest and next-nearest neighbors on the Fe hyperfine field in Fe–Cr alloys

is well known [43]. Thus the components in Mössbauer spectra of Fe/Cr multilayers [44] and thin Fe films on Cr(110) [45] have been straightforwardly attributed to the Fe local arrangements near the interfaces. The arrangements were found as characterized by various number of Cr nearest neighbors corresponding not only to a Fe/Cr sharp interface, but to the Fe film interior and to Fe step atoms at the interface as well. Relative contribution of the components, i.e., the sharpness of the interface, was found as strongly dependent on the preparation conditions. This means that CEMS can be used to follow the structural sharpness of the interfaces at the atomic scale, in particular if the ^{57}Fe probe layer method is applied. Then B_{hf} could be followed layer-by-layer in the absence of interior bulk-like components usually dominating the integral spectra of the films (due to a dominant contribution of the film interior to the film volume). In a case of ideal interface, it applies even if B_{hf} does not differ remarkably between the atomic layers and the corresponding components of integrated Mössbauer spectra remain unresolved. An example, using the ^{57}Fe probe layer method the increase in B_{hf} (above the bulk value) for the semi-infinite Fe/Ag and Fe/Au interfaces was found (in comparison to 30% reduction at the W/Fe interface) [46]. However, in all cases the B_{hf} approaches the bulk value already in the third atomic layer below the interface. The influence of noble metals on the magnetic hyperfine field in the topmost Fe layer

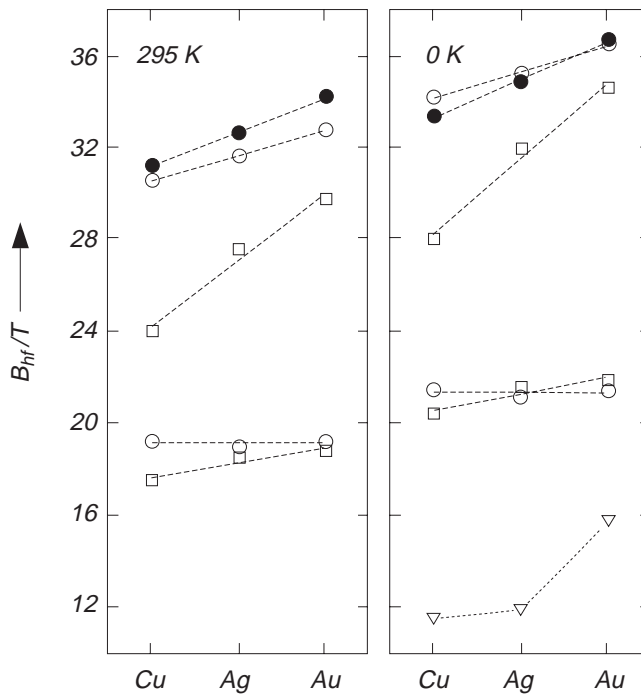


Figure 7. Magnetic hyperfine fields in the Fe/noble metal interfaces of: ● – 21-layer, ○ – 3-layer, □ – double-layer and ▽ – monolayer thick Fe films. For 3-layer, 2-layer and 1-layer film the values of B_{hf} for W/Fe interface are included (taken from [46]).

becomes stronger as film thickness is reduced (figure 7). Note that at finite temperatures the film magnetization decreases, and consequently the b parameter increases, with the reduction of the film thickness (this is why the relations shown in figure 7 are different at RT and 0 K). The constant value of $B_{\text{hf}}(0)$ in the interfaces with various metals down to the thickness of 3 ML leads to the conclusion that the thickness of three atomic layers is sufficient for the electronic structure in the interface to be influenced by the interfacing metal qualitatively and quantitatively in the same way as in a semi-infinite sample. This is not surprising because the nearest and next-nearest neighborhood of interfacial Fe atoms remains unchanged down to the thickness of three atomic layers. The short range modification of the band structure near the interface is contrary to the modification of the long range magnetic order which approaches the bulk-like level only inside a 40-layer thick Fe film [21,47].

4. fcc-Fe on Cu(001)

Defect-induced properties of thin films caused by mechanical interaction with the epitaxial substrate interfere with their intrinsic magnetic properties [48]. The most fascinating application of epitaxy is a possibility to stabilize crystallographic phases of material which do not exist naturally in a bulk form. In each of the different crystallographic structures magnetic metal exhibits different magnetic properties. Expansion or contraction of the atomic spacing as well as changed crystallographic symmetry influences band hybridization resulting in the local changes of the energy band structure. According to a general rule the greater the atomic distances are, the stronger the magnetism of Fe is. Thus, one can expect Fe grown on fcc-Cu(001) or hcp-Ru(0001) to be in a high-spin state due to the lattice expansion by about 1% and 13% in comparison with bcc-Fe, respectively.

The structural and magnetic properties of the fcc-Fe still remain a controversial topic. fcc-Fe which does not occur naturally can be stabilized in a form of Fe precipitates into fcc-matrix or as thin film grown on a fcc-substrate (e.g., on Cu(001)). Despite of the last development in production of epitaxial systems, the experimental data on the fcc-Fe-films structure still vary for preparations at different laboratories. In most cases they cannot be directly correlated with the magnetic properties of the films prepared elsewhere. This is not surprising taking into account that fcc-Fe is unstable in a bulk and metastable in a form of thin film. The direction of magnetization is unstable due to a competition between shape and surface anisotropy which depends strongly on film morphology resulting from the preparation conditions. Moreover, magnetic order is very sensitive to a lattice parameter in this system [49].

It is widely accepted that the Fe films on Cu(001) remain non-magnetic below 1.5 ± 0.2 monolayers independently of the preparation temperature. In the 2–5 ML thickness range, the films prepared at room temperature and below show ferromagnetic order with a saturation magnetization increasing proportionally to the increasing film thickness. The magnetization direction is reported to be perpendicular to the film

plane in both cases. With increasing film thickness the magnetization switches to in-plane. For the films prepared at low temperature (resulting in very rough surfaces of the films), the switching proceeds at a thickness of 5–6 monolayers. A roughness-induced modification of the effective uniaxial surface anisotropy supports the changes in macroscopic shape anisotropy responsible for the magnetization switching. For the films prepared at room temperature, at the same thickness of 5–6 ML the saturation magnetization drops but its direction remains perpendicular to the film plane. This effect coincides with a different size of the domains which are of two orders of magnitude larger in the films prepared at low temperature in comparison with that prepared at RT. It is surprising that the magnetic moment does not change up to the thickness of about 10 ML. Above 10–11 ML the films are continuous and thick enough to become unstable toward the fcc–bcc phase transition [49].

Onset of ferromagnetism in the Fe/Cu(001) system is “delayed” in this sense that ferromagnetic order is not established at its percolation threshold. For the films deposited at RT, experimentally observed ferromagnetic onset is at 1.5 ML, whereas the first layer percolates already at 0.9 ML. It is contrary to bcc-Fe submonolayer on W(110) system in which the transformation from the superparamagnetic to the ferromagnetic behavior occurs just at the percolation limit. Several reasons are supposed to be responsible for such the “delay” [49]:

- intermixing between Fe and Cu atoms is not suppressed even if the films are prepared at relatively low temperatures; the same property is reported for Fe submonolayer on W(110) coated with Cu – just annealing up to the room temperature changes the local atomic arrangement irreversibly,
- a nearest neighbor distance between Fe atoms is reduced by 7% in comparison with that of Fe atoms in the submonolayer-Fe/W(110) system,
- strong uniaxial in-plane anisotropy caused by 2-fold symmetry of the bcc(110) surface (to be compared with 4-fold symmetry of fcc(100) surface) may additionally stabilize the ferromagnetic order in a Fe/W(110) system,
- a nearest neighbor coordination of surface atoms for bcc(110) and fcc(001) surfaces is different (number of magnetic neighbors equals 6 and 4, respectively) [49].

The percolation limit at 0.9 ML for Fe on Cu(001) can be compared with the value of 0.6 ML which was found for Fe on W(110). At RT, Fe growth on Cu(001) is characterized as a “disordered” in the initial stages, instead of a nearly perfect layer-by-layer growth reported for Fe on W(110) in the same coverage range. Quite recently the Pulsed Laser Deposition (PLD) method was found as a useful technique to force layer growth of Fe on Cu(001) in monolayer thickness range. The Fe atoms deposited in the PLD process have a higher energy that enhances a mobility of the atoms resulting in the increased nucleation probability [50]. Thus the morphological percolation is expected to occur at the much lower coverage. With reference to Fe on W(110), CEMS seems to be a promising technique to study the detailed correlation between the local atomic arrangement and the onset of magnetic order in the thinnest Fe films on Cu(001) and

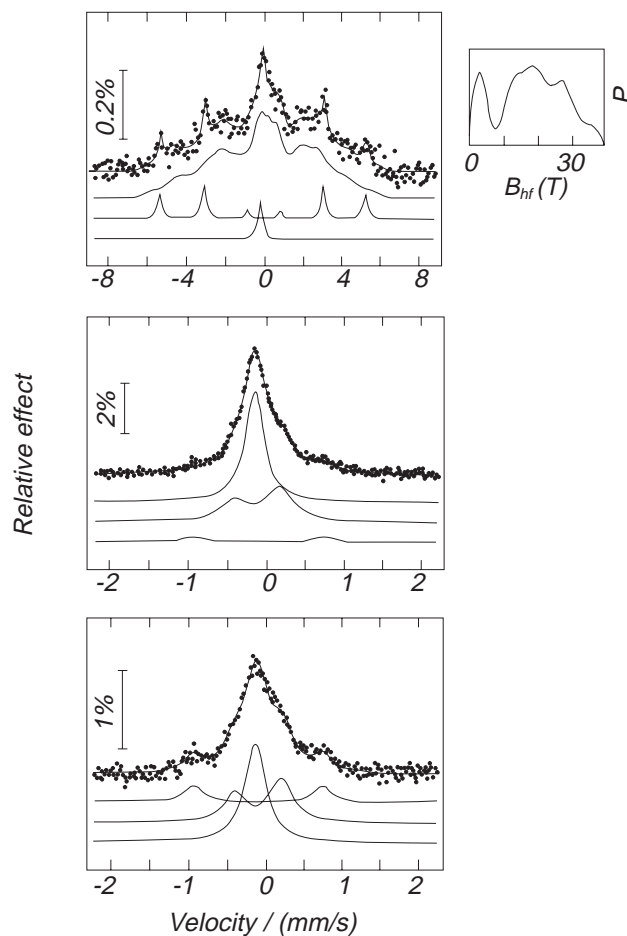


Figure 8. ^{57}Fe probe monolayer CEMS spectra measured at 300 K of 300 K grown ^{57}Fe probe layer (2 ML) in natural Fe/Cu(001) film, 7-layer thick in total. ^{57}Fe is placed on top of the film (upper spectrum), in the film center (central spectrum) and at the Cu(001)/Fe interface (bottom spectrum) (taken from [56]).

Cu(111). Fe on Cu(111) seems to be even more exciting concerning “decoration” of the Cu terrace edges in this case [50]. It is possible to prepare submonolayer of Fe on a vicinal Cu(111) surface in a form of quasi one-dimensional structures (wires) elongated through the edges if they are sufficiently narrow [51]. The wires are similar to that observed for Fe grown on W(110) at elevated temperatures and have the same superparamagnetic behavior [51].

Independence of magnetic moment of the film thickness remains a point of controversy for a long time. Two interpretations are proposed [49]:

- only surface layers are ferromagnetic; layers below the surface are magnetically dead [52] or they exhibit antiferromagnetic order [53],

- some structural transformation from a tetragonally distorted (fct) to a more perfect fcc structure exists; forthcoming atomic layers of fcc-symmetry do not participate to the magnetic moment already determined (fct-Fe is ferromagnetic).

Just recently it has become commonly accepted that an undistorted fcc structure exists in the interior of the 5–10 ML thick films and is identified as a low-spin antiferromagnetic phase. However, the interlayer distance close to the surface is expanded (relaxed) and therefore responsible for the observed ferromagnetism in the surface layer. Reliable experimental results concerning “magnetic live layers” come from the Magnetization Induced Second Harmonic Generation experiment, which provides a definite location of magnetization at the surface only [54]. For Fe on Cu(001) films in the 5–10 ML thickness range a complex Mössbauer study does not exist. Only available are the data on a 7 ML film reported by Keune et al. [55,56]. Evidence of antiferromagnetic magnetic order in this case is provided by a broadening of the fcc-Fe single line at low temperatures. Magnetically live layers are found with so called “site-selective” CEMS which is actually ^{57}Fe monolayer probe method. Figure 8 shows the spectra of the films with 2 monolayers of various positions replaced with ^{57}Fe . At the surface the dominant spectral contribution involves a very broad distribution ranging from 10 to 35 T with an average field of $B_{\text{hf}} = 18$ T. These atoms are in a high-spin state which is probably ferromagnetic. The B_{hf} distribution of the surface does not appear in the spectra for the films with ^{57}Fe layers deposited at the center or at the Cu/Fe interface. Interesting is that although the measurement time was rather long and the surface was coated with residual gas atoms, surface magnetism is not suppressed in this case.

5. hcp-Fe on Ru(0001)

Contrary to the expectation that expanded atomic distances stabilize ferromagnetic order, the nonmagnetic Fe layers near the Ru/Fe interface were observed by Maurer et al. [57] and by us [58,59]. Dealing with the available experimental data one can conclude that the structure of the Fe grown on Ru depends on a rate of growth [60]. For a high growth rate (more than $30 \text{ \AA}/\text{min}$) the hcp structure was found to occur in FeRu superlattices up to 14 \AA of Fe. For a lower evaporation rate ($1\text{--}2 \text{ \AA}/\text{min}$), Fe tends to relax to a more stable bcc-Fe. Nevertheless, the first 1–2 Fe atomic layers are always pseudomorphic to the substrate. They are of hexagonal symmetry and seem to be non-magnetic. Therefore, the hcp-structure (or, at least, hexagonal symmetry combined with expanded atomic distances) of Fe atoms was suggested to be responsible for vanishing of the magnetic moment contrary to the general expectation. Non-magnetic Fe atoms were found near the interface between bcc-Fe and Ru-overlayer [58]. Such situation corresponds to a high efficiency of Ru to destroy the Fe magnetism due to a strong hybridization between 3d-Fe and 4d-Ru electronic bands [61]. Nevertheless, at least two phenomena caused by the forthcoming Ru overlayer could be crucial for the structure of interface and can significantly influence its magnetic properties: rearrangement of Fe atomic positions and interlayer mixing between Fe and Ru. Particularly,

surface alloying could be associated with local changes of the crystallographic structure. It was shown before that the “substrate-Ru”/Fe and Fe/“Ru-overlayer” interfaces are not equivalent. At low temperature the hcp-like-Fe-phase at “substrate-Ru”/Fe interface undergoes the transition from a paramagnetic state to a low spin antiferromagnetic state, analogous to that observed in Fe films on Cu(001). Such an effect is not observed in the Fe/“Ru-overlayer” interface. Thus the difference between “Ru-substrate”/Fe and Fe/“Ru-overlayer” is supposed to correspond to the hexagonal and bcc symmetry of Fe interfacing atomic layers, respectively. In order to find out if the magnetic and structural behavior of the uncovered surface of thick (30-layers) Fe film are that of the bcc-Fe, the Mössbauer spectra were measured (for the film of 28 layers of ^{56}Fe and two topmost layer of ^{57}Fe , see figure 9). It became clear that: (i) top atomic layers of Fe are ferromagnetic, (ii) they reveal bcc(110) structure (the spectra

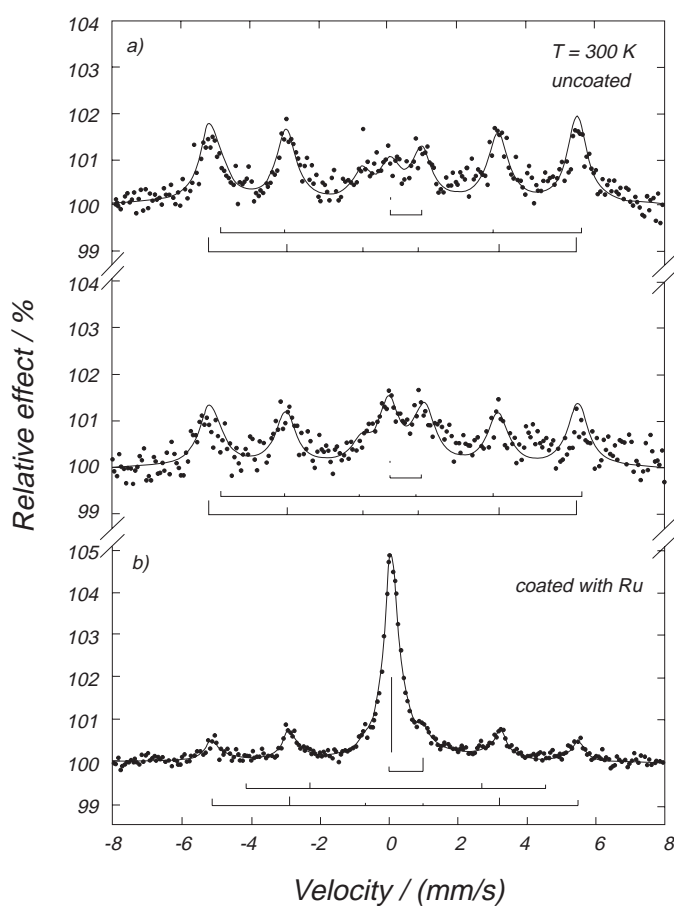


Figure 9. Mössbauer spectra of 2 ML of ^{57}Fe deposited on the top of a 30 ML of ^{56}Fe . (a) The upper spectrum was measured for 24 hours starting just after preparation. The bottom spectrum was measured for the next 24 hours. (b) Mössbauer spectra of the same sample which was coated with 50 Å of Ru 48 hours after deposition of Fe (taken from [59]).

components were fitted with the parameters similar to those reported previously for bcc-Fe(1 1 0) surface [18,19]). After covering of the film with Ru, remarkable changes in the CEMS spectrum were observed as seen in figure 9. The spectrum became mainly “non-magnetic” and very similar to that measured for the Fe film coated with Ru immediately after deposition of Fe [58]. The bulk-like component in the spectrum, with the value of the magnetic hyperfine field close to that of α -Fe, corresponds to the ^{57}Fe atoms with only Fe atoms as the nearest neighbors. The second component is due to the distribution of magnetic hyperfine field caused by a various number of Ru atoms sitting in the positions of nearest neighbors. The relatively low fields (about 26 T) are due to local Fe coordination for which the number of the nearest and the next nearest Ru neighbors exceeds the maximum value possible for the bcc alloys of the maximal Ru concentration. The third component, which is a quadrupole doublet, is supposed to be due to the Fe atoms that are surrounded by the atoms of residual gases adsorbed on the surface exposed to UHV for 48 hours (time of measurement). The fourth component, most intensive, is a single line which is assumed to correspond to the Fe atoms surrounded by a number of Ru atoms being sufficient to destroy the Fe magnetism. Consequently, we propose that the origin of the single line found in our spectra has nothing to do with the local hexagonal structure of the film. The collapse of the magnetic hyperfine field is connected with a large number of Ru atoms in the nearest neighborhood of Fe atoms. Some arguments support the interpretation. In the case of FeRu alloys or Fe_xRu_y superlattices of the hexagonal structure, the characteristic quadrupole doublet in Mössbauer spectra is always observed instead of the single line. There is a distinct difference between the values of the isomer shift in the Fe/“Ru-overlayer” interfaces and that in the “Ru-substrate”/Fe [58,59]. Finally, to our opinion the electronic interactions (strong hybridization between Fe and Ru d-bands), rather than the hcp-like structural modification, are responsible for the quenching of the hyperfine magnetic field in Fe/Ru interface. Any evidence of an existence of hcp-Fe was found except of eventually hcp-like symmetry in the first atomic layer pseudomorphic to the Ru(000 1) substrate.

6. Multilayers

Artificially structured metallic multilayers have attracted great attention in the past decade. This is due to the giant magnetoresistance phenomena and interlayer exchange couplings between magnetic layers through non-magnetic spacer firstly reported by Grünberg et al. [63] and Baibich et al. [64]. In a simple phenomenological approach, if the magnetization of ferromagnetic layers (separated with non-magnetic spacer) are aligned antiparallel all conduction electrons pass interfaces with magnetization in opposite direction and all of them are scattered. If the magnetic layers are aligned parallel, the conduction electrons have a long mean free path and the total resistivity is much smaller. However, the actually observed changes in resistivity (caused by the antiparallel magnetic structure) are much larger than expected. Some experimental results confirm that the giant magnetoresistance is not only related to the parallel or

anti-parallel interlayer coupling, but to much more complicated mechanisms of the interlayer exchange interaction. Systematic studies of various multilayers found that the oscillations with a period of about 10 ML is a general feature. Additionally existing short-range oscillation of interlayer coupling with a period of two atomic distances are explained by the RKKY mechanism [65].

Mössbauer spectroscopy has been successfully applied for the studies of interlayer coupling for a long time. The induced spin polarization in the non-magnetic separating layer can be observed, if a Mössbauer probe exists there. However, ^{57}Fe is not appropriate in this case, because doping of Fe magnetic atoms perturbs the magnetic behavior of a non-magnetic layer. Non-magnetic ^{119}Sn seems to be a much better choice in this case [65].

If the interlayer coupling strength is comparable to the anisotropy energies of the system, it is possible that antiferromagnetic oscillations are very weak and cannot be detected by magnetometric methods. The only method to analyze the character of the exchange coupling is to measure the spin-wave spectrum. In particular, this can be done by ^{57}Fe Mössbauer spectroscopy. Information can be obtained by measuring the $T^{3/2}$ prefactor b in the Bloch law describing the temperature dependence of magnetization (and magnetic hyperfine field). If $B_{\text{hf}}(T)$ is followed in the interface with a non-magnetic spacer of variable thickness, b reflects the interfacial spin-wave modes which are alternately softened and stiffened with oscillating interlayer exchange [66].

An interface roughness is essential for the spin-dependent scattering (however, it is not yet clarified whether the scattering occurs at the interface or in a magnetic layer). CEMS studies of ^{57}Fe probe atoms inserted at various distances from the interface establish the suitability of the technique for obtaining information on interdiffusion and interface roughness on an atomic scale. Use is made of the fact that the hyperfine field is predominantly determined by the environment of nearest- and next-nearest-neighbor atoms. Since the discovery of indirect exchange coupling between two Fe layers separated by a Cr spacer, the Fe/Cr/Fe is the most often studied system in the field of nanostructures (e.g., [67]). The exchange coupling through the Cr film oscillates as a function of spacer thickness. The oscillations have two characteristic wavelengths: 2.11 and 12 ML. The presence of the short-wavelength oscillation in the exchange coupling is predicted theoretically by *ab initio* calculations as a result of a spin-density wave of the same wavelength in bulk Cr. The spin-density waves are predicted to be antiferromagnetically coupled with Fe at both of the interfaces, i.e., the coupling through the Cr spacer should be antiferromagnetic for an even number of atomic layers. Contrary to this expectation the opposite phase of the oscillations is found experimentally (e.g., [68]). Recently, two experiments were performed in order to explain this reversed phase of short wavelength oscillations compared to those predicted by calculations. Angle resolved Auger electron forward scattering was applied to analyze the chemical state of the Fe substrate after deposition of 0.5 monolayers of Fe at different temperatures [69]. The results indicate significant intermixing of Cr atoms into the second layer of Fe and likely also to the third one. In the “chemically sensitive” STM experiment performed by Davies et al. [70] it is shown that Cr growth

on a Fe(001) surface under layer-by-layer conditions leads to the formation of a Cr-Fe alloy. Some of deposited atoms of Cr replace Fe atoms and the growing layer contains mostly Fe. It is shown that only one of every four Cr atoms deposited on Fe remains in the surface layer. In both experiments the interface alloying at the Fe/Cr interface is suggested to be responsible for the reversed sign and strength of the exchange coupling through the Cr spacer. Samples prepared by simultaneous deposition of both elements (Fe and Cr) at elevated temperature result in a clear sign reversal of the exchange coupling.

Nevertheless, some aspects of the interface alloying still remain unclear. Firstly, how does the process look like if the Fe surface is coated with much more than 0.5 monolayer of Cr? Some experimental evidence exists (e.g., for Fe/Al interfaces [71]) that the diffusion depends on the individual layer thickness of both interfacing elements. Secondly, how does the process depend on the rate of growth? A competition between a rate of alloying and the probability of meeting a Cr atom by another Cr atom exists. At high growth rate the Cr atoms can form small clusters which are suggested to retard the alloying process. No quantitative identification of the preferred atomic coordination (e.g., similar to that of the ordered alloys) is possible using AES and STM. Actually the problem concerns the local magnetic properties related to the local atomic arrangements caused by alloying in the broadened interface region. Mössbauer spectroscopy appears to be an extremely convenient tool for this purpose since both structural and magnetic information can be achieved.

Recently, layered structures not occurring naturally neither as alloy nor as intermetallic compounds have been fabricated artificially. A certain degree of ordering ($L1_0$ type FeAu) has been obtained for the AuFe superlattice [72]. The paper concerning their magnetic and structural properties is published in the Proceedings of this conference [73].

Acknowledgements

I gratefully acknowledge cooperation and many helpful discussions with Prof. U. Gradmann, Prof. B. Heinrich, Prof. J. Kirschner and Prof. J. Korecki.

The paper was written in part during my stay at Max-Planck-Institut für Mikrostrukturphysik at Halle, Germany. I wish to acknowledge the invitation of Prof. J. Kirschner and the support of Max-Planck-Gesellschaft.

This work was supported by the Polish Science Research Council, Grant No. 2P03B 08010.

References

- [1] C. Li and A.J. Freeman, Phys. Rev. B 43 (1991) 780.
- [2] W. Döring, Z. Naturforschung 16a (1961) 1008.
- [3] H. Fritzsche, H.J. Elmers and U. Gradmann, J. Magn. Mater. 135 (1994) 343.
- [4] H.J. Elmers and U. Gradmann, Surf. Sci. 304 (1994) 201.

- [5] L. Néel, J. Phys. Radium 15 (1954) 225.
- [6] B. Heinrich and J.A.C. Bland, eds., *Ultrathin Magnetic Structures I and II* (Springer-Verlag, Berlin, 1994).
- [7] M. Przybylski and U. Gradmann, J. Physique C 8 (1988) 1705.
- [8] E. Bauer, Kristall. Z. 110 (1958) 372.
- [9] I. Markov and R. Kaischew, Kristall und Technik 11 (1976) 685.
- [10] E. Kisker, K. Schröder and W. Gudat, Phys. Rev. B 31 (1985) 329.
- [11] S.D. Bader, J. Magn. Magn. Mater. 100 (1991) 440.
- [12] U. Gradmann and R. Bergholz, Phys. Rev. Lett. 52 (1984) 771.
- [13] G. Schatz, in: *Proc. of Zakopane School on Physics*, Zakopane, 1991 (World Scientific, Singapore, 1991).
- [14] P. Panissod, J.P. Jay, C. Meny, M. Wojcik and E. Jedryka, Hyp. Interact. 97/98 (1996) 75.
- [15] G. Bayreuther, J. Magn. Magn. Mater. 38 (1983) 273.
- [16] M. Przybylski, I. Kaufmann and U. Gradmann, Phys. Rev. B 40 (1989) 8631.
- [17] G. Catchen, MRS Bull. 7 (1995) 37.
- [18] J. Korecki and U. Gradmann, Phys. Rev. Lett. 55 (1985) 2491.
- [19] J. Korecki, *Surface, Interface and Thin Film Magnetism of Iron as Seen by Mössbauer Spectroscopy* (AGH, Krakow, 1991).
- [20] Z. Kajcosos, W. Meisel, P. Griesbach, P. Gutlich, M.A.C. Lightenberg, U. Gradmann, E. Lehrberger and M. Przybylski, Hyp. Interact. 71 (1992) 1483.
- [21] M. Przybylski, *From Three- to Two-Dimensional Magnetism of Fe* (AGH, Krakow, 1997).
- [22] D. Liljequist, Phys. Rev. B 31 (1985) 4131.
- [23] M. Przybylski, in: *Proc. of Zakopane School on Physics*, Zakopane, 1993, eds. E. Görlich and K. Tomala (UJ, Krakow, 1993) p. 97.
- [24] J. Korecki and U. Gradmann, Europhys. Lett. 2 (1986) 651.
- [25] U. Gradmann, M. Przybylski, H.J. Elmers and G. Liu, Appl. Phys. A 49 (1989) 563.
- [26] M. Przybylski and U. Gradmann, Phys. Rev. Lett. 59 (1987) 1152.
- [27] H.J. Elmers, J. Hauschild, H. Fritzsche, G. Liu, U. Gradmann and U. Köhler, Phys. Rev. Lett. 75 (1995) 2031.
- [28] N. Weber, K. Wagner, H.J. Elmers, J. Hauschild and U. Gradmann, Phys. Rev. B (1997).
- [29] T. Dürkop, H.J. Elmers and U. Gradmann, J. Magn. Magn. Mater. 172 (1997) L1.
- [30] Y. Park, S. Adenwalla, G.P. Felcher and S.D. Bader, Phys. Rev. B 52 (1995) 12779.
- [31] T.B. Massalski, ed., *Binary Alloy Phase Diagrams*, 2nd edn. (ASM International Metals Park, OH, 1990).
- [32] M. Przybylski, J. Prokop, P. Auric and J. Korecki, in: *Proc. of the 10th Int. Conf. on Hyperfine Interactions*, Leuven, Belgium, 1996, Hyp. Interact., part II, p. 314.
- [33] F. Huang, G.J. Mankey, M.T. Kief and R.F. Willis, J. Appl. Phys. 73 (1993) 6760.
- [34] M. Przybylski, J. Korecki and U. Gradmann, Appl. Phys. A 52 (1991) 33.
- [35] D. Sander, R. Skomski, C. Schmidhals, A. Enders and J. Kirschner, Phys. Rev. Lett. 77 (1996) 2566.
- [36] H. Bethge, D. Heuer, Ch. Jensen, K. Reshoeft and U. Köhler, Surf. Sci. 331–333 (1995) 878.
- [37] H.J. Elmers and J. Hauschild, Surf. Sci. 320 (1994) 134.
- [38] H.J. Elmers, J. Hauschild, H. Hoche, U. Gradmann, H. Bethge, D. Heuer and U. Köhler, Phys. Rev. Lett. 73 (1994) 898.
- [39] R. Wu and A.J. Freeman, Phys. Rev. B 45 (1992) 7532.
- [40] S.C. Hong, A.J. Freeman and C.L. Fu, Phys. Rev. B 38 (1988) 12156.
- [41] M. Przybylski, U. Gradmann and J. Korecki, J. Magn. Magn. Mater. 69 (1987) 199.
- [42] U. Gradmann and M. Przybylski, in: *Thin Film Growth Technique. Magnetic Interface Preparation and Analysis*, eds. R. Farrow, S. Parkin, P.J. Dobson, J. Neave and A. Arrott (Plenum Press, New York, 1987) p. 261.

- [43] S.M. Dubiel and W. Zinn, *Phys. Rev. B* 30 (1984) 3783.
- [44] J. Landes, C. Sauer, R.A. Brand, W. Zinn, S. Mantl and Zs. Kajcsos, *Hyp. Interact.* 86 (1990) 1941.
- [45] J. Zukrowski, G. Liu, H. Fritzsche and U. Gradmann, *J. Magn. Magn. Mater.* 145 (1995) 57.
- [46] M. Przybylski, J. Korecki, W. Karas and U. Gradmann, in: *Proc. of ICAME '95*, *Nuovo Cimento* 50(II) (1996) 611.
- [47] G. Liu and U. Gradmann, *J. Magn. Magn. Mater.* 118 (1993) 99.
- [48] J.W. Matthews and E. Klokholm, *MRS Bull.* 7 (1972) 213.
- [49] J. Giergiel, J. Shen, J. Woltersdorf, A. Kirilyuk and J. Kirschner, *Phys. Rev. B* 52 (1995) 8528.
- [50] H. Jenniches, M. Klaua, H. Hoche and J. Kirschner, *Appl. Phys. Lett.* 69 (1996) 3339.
- [51] J. Shen, R. Skomski, M. Klaua, H. Jenniches, S. Sundar Manoharan and J. Kirschner, *Phys. Rev. B* 56 (1997) 2340.
- [52] J. Thomassen, F. May, B. Feldmann, M. Wuttig and H. Ibach, *Phys. Rev. Lett.* 69 (1992) 3831.
- [53] D. Li, M. Freitag, J. Pearson, Z.Q. Qiu and S.D. Bader, *Phys. Rev. Lett.* 72 (1994) 3112.
- [54] R. Vollmer, M. Straub and J. Kirschner, *Surf. Sci.* 352–354 (1996) 684.
- [55] R.D. Ellerbrock, A. Fuest, A. Schatz, W. Keune and R.A. Brand, *Phys. Rev. Lett.* 74 (1995) 3053.
- [56] W. Keune, A. Schatz, R.D. Ellerbrock, A. Fuest, K. Wilmers and R.A. Brand, *J. Appl. Phys.* 79 (1996) 4265.
- [57] M. Maurer et al., *J. Magn. Magn. Mater.* 93 (1991) 1524.
- [58] M. Przybylski, J. Prokop, P. Auric and J. Korecki, in: *Proc. of ICAME '95*, *Nuovo Cimento* 50(II) (1996) 599.
- [59] J. Prokop, M. Przybylski, T. Slezak and J. Korecki, *Surf. Rev. Lett.* 4 (1997) 1239.
- [60] S. Andrieu, M. Piecuch and J.F. Bobo, *Phys. Rev. B* 46 (1992) 4909.
- [61] D. Knab and C. Koenig, *Phys. Rev. B* 43 (1991) 8370.
- [62] J. Korecki and U. Gradmann, *Phys. Rev. Lett.* 55 (1985) 2491.
- [63] P. Grünberg, R. Schreiber, Y. Pang, M.B. Brodsky and H. Sowers, *Phys. Rev. Lett.* 57 (1986) 2442.
- [64] M.N. Baibich, J.M. Broto, A. Fert, F. Nguyen Van Dau, F. Petroff, P. Etienne, G. Creuzet, A. Friederich and J. Chazelas, *Phys. Rev. Lett.* 61 (1988) 2472.
- [65] T. Shinjo, in: *Proc. of ICAME '93*, Vancouver, 1993, *Hyp. Interact.*
- [66] J.W. Freeland, D.J. Keavney, D.F. Storm, I.L. Grigorov and J.C. Walker, *Phys. Rev. B* 54 (1996) 9942.
- [67] F. Klinkhammer, Ch. Sauer, E.Yu. Tsybal, S. Handschuh, Q. Leng and W. Zinn, *J. Magn. Magn. Mater.* 161 (1996) 49.
- [68] B. Heinrich, M. From, J.F. Cochran, M. Kowalewski, D. Atlan, Z. Celinski and K. Myrtle, *J. Magn. Magn. Mater.* 140–144 (1995) 545.
- [69] D. Venus and B. Heinrich, *Phys. Rev. B* 53 (1996) R1733.
- [70] A. Davies, J.A. Stroschio, D.T. Pierce and R.J. Celotta, *Phys. Rev. Lett.* 76 (1996) 4175.
- [71] A.R. Chowdhury and A.E. Freitag, *J. Appl. Phys.* 79 (1996) 6303.
- [72] S. Mitani, K. Takanashi, H. Nakajima, K. Sato, R. Schreiber, P. Grünberg and H. Fujimori, *J. Magn. Magn. Mater.* 156 (1996) 7.
- [73] T. Slezak, W. Karas, M. Kubik, M. Mohsen, M. Przybylski, N. Spiridis and J. Korecki, in: *Proc. of ICAME '97*, *Hyp. Interact.*